ISSN: 0067-2904

Investigation of Aluminum Arsenide Honeycomb Monolayer via Density Functional Theory

Aqeel Mohsin Ali
Material Science Department, Polymer research Center, University of Basrah, Basrah, Iraq

Received: 10/3/2022 Accepted: 24/6/2022 Published: 30/1/2023

Abstract

First principle calculations are performed to theoretically predict the physical properties of hexagonal aluminium arsenide planar and buckled monolayers. The structural characteristics showed that the buckled parameter is about 0.32 A°. Cohesive energies have favourable values and it indicates the fabrication possibility. Phonon dispersion properties indicated that the planar aluminium arsenic monolayers are dynamically unstable, while the buckled is less dynamically unstable. The elastic constant parameters achieved the required characteristics of stable hexagonal monolayer structures. The study of electronic band structure prefers to indirect semiconductor band gaps, and the density of states showed strong orbital hybridization in the conduction band. Planar structure has isotropic light electron effective mass and anisotropic heavy hole effective mass. The buckled structure has isotropic light electron effective mass and isotropic heavy hole effective mass. The absorption spectra have high absorption coefficient in various visible and ultraviolet wavelength. The absorption coefficient levels off at about direct and indirect band gaps.

Keywords: Density functional theory; Hexagonal AlAs monolayer; Elastic properties, electronic properties; absorption.

أستقصاء المنيوم ارسينايد أحادي الطبقة شكل خلية النحل أعتمادا على نظرية دالة الكثافة

عقيل محسن علي
قسم علوم المواد, مركز أبحاث البوليمر , جامعة البصرة, محافظة البصرة, العراق

الخلاصة

أجريت حسابات من المبادئ الاولية للتكهن نظريا بالخصائص الفيزيائية للالمنيوم أرسينايد ألسداسي أحادي الطبقة المستوية أو المنبعجة. أظهرت المميزة التركيبية أن معلم ألانبعاج كان بحدود 0.32 A° . تمتلك طاقات التماسك قيما مؤاتية وتشير الى أمكانية تصنيعها. أظهرت خصائص التفريق للفونونات أن ألالمنيوم أرسينايد أحادي الطبقة المستوي غير مستقر ديناميكيا، بينما التركيب المنبعج يبدو غير مستقر ديناميكيا بشكل طفيف. تحقق معلمات ثابت المرونة ما هو مطلوب في مميزات التركيبات المستقرة أحادية الطبقة السداسية. أشارت دراسة حزم الطاقة الالكترونية الى فجوات الطاقة غير المباشرة لاشباه الموصلات، و بينت كثافة الحالات وجود تداخل قوي بين المدارات في حزمة التوصيل. يمتلك التركيب المستوي كتلة فعالة للالكترونات منتظمة و خفيفة، و كتلة فعالة للفجوات ثقيلة غير منتظمة. يمتلك التركيب المنبعج كتلة فعالة للالكترونات

*Email: aqeel.mohsin@uobasrah.edu.iq

منتظمة و خفيفة، و كتلة فعالة للفجوات ثقيلة و منتظمة. بين طبف ألامتصاص معامل أمتصاص عالي للأطوال الموجية المرئية وفوق البنفسجية. تنطلق مستويات معاملات الامتصاص من قيم فجوات الطاقة المباشرة وغير المباشرة.

1. Introduction

The successful fabrication of graphene in 2004 has led to the discovery of various two-dimensional materials beyond carbon [1, 2]. Several groups IV monolayers, such as silicene, stanene, and germanene, have been proposed by various investigations. These have been characterized and synthesized, and their measured electronic and structural properties have been confirmed. The computational studies conducted on the various 2D compounds and crystal structures have led to the discovery of various groups III, V, VI, and VII monolayer materials [3]. They have also shown promising results in developing high-performance electronic devices and optoelectronics. More than 1500 2D materials have been studied and recorded in the database, which have revealed promising applications in electronic devices. 2D hBN is widely used as an insulating layer to form strong and stable contact with other 2D materials. Theoretically, various types of square-octagon III-V and hexagonal III-V monolayers have also been studied. The computational design of the semiconductor has revealed its usefulness in multiple applications, such as batteries [4, 5].

A novel phase-based orthorhombic BN, which exhibits exceptional electronic properties, has been proposed. It has been widely used in optoelectronic devices due to its excellent stability and structural properties. More recently, the various optical and electronic properties of these monolayers have been examined [6]. The atomic structures of the III-V orthorhombic single layers are characterized by the bonds connecting the V and III sides to form a unit cell. Theoretical results have revealed that the bandgaps of various materials, such as 2D BN, AlN, and GaN, are suitable for their anisotropic absorbance and solar spectrum. These materials are expected to play a significant role in the development of anisotropic optoelectronic devices. In a recent study using first-principles plane waves, Sahin et al. compared the stability of 2D planar GaAs to low buckled GaAs using the honeycomb structure. They found that the 2D planar GaAs structure is less stable [7]. Notably, a monolayer of AlN nano-sheets was successfully synthesized, following the theoretical predictions [8, 9]. This opened up several other possibilities for this group [10, 11]. A comprehensive theoretical analysis of the physical properties of aluminium arsenide AlAs must still be explored and studied, even though AlN and GaAs have been extensively studied recently [7, 10].

Among the most studied useful semiconductors, is aluminium arsenide (AlAs) which has a 2.15 eV indirect band-gap [12, 13]. It has been used in lasers [14], light-emitting diodes [15], photo-detectors [16], and electro-optic modulators [17]. It is important to theoretically predict band structures, fundamental energy gaps, and effective masses of semiconductors and alloys to fabricate hetero-structures and devices. The bulk aluminium arsenide (AlAs) is a well-studied semiconductor due to its potential applications in optoelectronic devices [17, 18], whereas 2D AlAs still have to turn a blind eye in both experimental and theoretical studies. The window of opportunity is wide open to invest and explore a new graphene-like monolayer aluminium arsenide (MAlAs). Although the above-mentioned work for GaAs can be applied to AlAs, it is a density functional theory (DFT) work, and as far as we know, the literature comes up short on an investigation beyond the DFT. So, in this work, it is intended to contribute theoretically to this topic. In this paper, first-principles calculations are performed within density functional theory (DFT) to find the stability, mechanical, optical and ground state band diagram of the buckled and planar AlAs monolayers.

2. Computational method

All computations introduced were acted in Materials Studio 4.0's CASTEP module, which was used to calculate the density functional theories. The total plane-wave pseudo-potential method drove the CASTEP calculations [19, 20]. Structure optimization, phonon calculations, and elastic constant calculations were performed based on a generalized gradient approximation (GGA) with Perdew-Burke-Ernzerhof (PBE) function [21]. Heyd–Scuseria–Ernzerhof functional (HSE06) level was used to explore the electronic structure and the absorption spectrum [22]. The self-consistent field quality was set as an ultrafine option. The Monkhorst–Pack scheme k-point grid sampling was set at 12 × 12 × 1 for the Brillouin zone. The plane-wave energy cut-off was set at 330 eV. Norm conserving pseudo-potentials and all band/EDFT electronic minimizer were used for all chemical elements. Geometry optimizations were carried out by the Broyden-Fletcher-Goldfarb-Shanno (BFGS) algorithm. Default values were set for the other calculation parameters as it was entered into CASTEP program. After optimizing the crystal structure, the band structures, the density of states and optical properties of all considered crystals were calculated. The buckled monolayer created by the plane (1 1 1) cuts all three crystallographic axes of the cubic crystal system F-43m of AlAs. The planar monolayer is built by the unit cell of a graphene crystal. For all computations, monolayer set corresponding to the a-b plane and normal direct c, and to avoid interlayer association with the length of super-cell being 50 A° a vacuum thickness was taken on.

3. Results

The honeycomb structure of the AlAs monolayer is created by ordering nine skeleton rings, with a single planar unit cell within the AlAs monolayer consisting of a single Al atom and a single As atom, while a single unit cell of buckled AlAs monolayer consists of three Al atoms beside a single As atom, as displayed in Figure 1. Table 1 presents all the structural parameters and mechanical and electronic properties. Optimization with full relaxation of all MAlAs atoms yields the equilibrium lattice constant as a = 4.03 and 4.01 A° of planar and buckled system, respectively. MAlAs buckling distance is 0.32 A° and Al-As bond length is about 2.34 A°.

It is necessary to theoretically check the stability and approve the possibility of fabricating AlAs monolayer before exploring the potential function of MAlAs. The first step was to determine the cohesive energy estimated by $E_{coh} = (E_{Al} + E_{As} - E_{MAlAS})/2$, where E_{Al} , E_{As} and E_{AlAs} are the total energy of a single Al, As atoms and AlAs unit cell, respectively. Planar and buckled MAlAs have favourable values of cohesive energies of ~ 5.06 eV. The value of cohesive energy as fixed in Table1, which indicates that it is between planar and buckled, gives an indication of the fabrication possibility of AlAs monolayer. The second step was the phonon dispersion investigation to evaluate the dynamical stability. Figure 2 shows the phonon band structure of planar and buckled MAlAs in Brillouin zone along the high-symmetry points (K→Γ→M). The phonon dispersion band structure possesses imaginary frequency modes, that clearly detect a kinetic instability of MAlAs. The buckled MAlAs is more stable than planar. Imaginary modes can be found only for buckled MAlAs at both K(-0.333 ; 0.667 ; 0.000) and M(0.000 ; 0.500 ; 0.000) points. Then, the buckled MAlAs structure is deformed along these directions.

According to this result, the buckled MAlAs is unstable at low temperatures. At proper high temperatures, large atomic displacements can stabilize the buckled MAlAs structure. In planar MAlAs case, high instability at the Γ point leads to difficult experimental synthesis,

and it will be transformed into a buckled structure, which is dynamically less unstable. Planar MAlAs structure system occurs at higher temperatures [9].

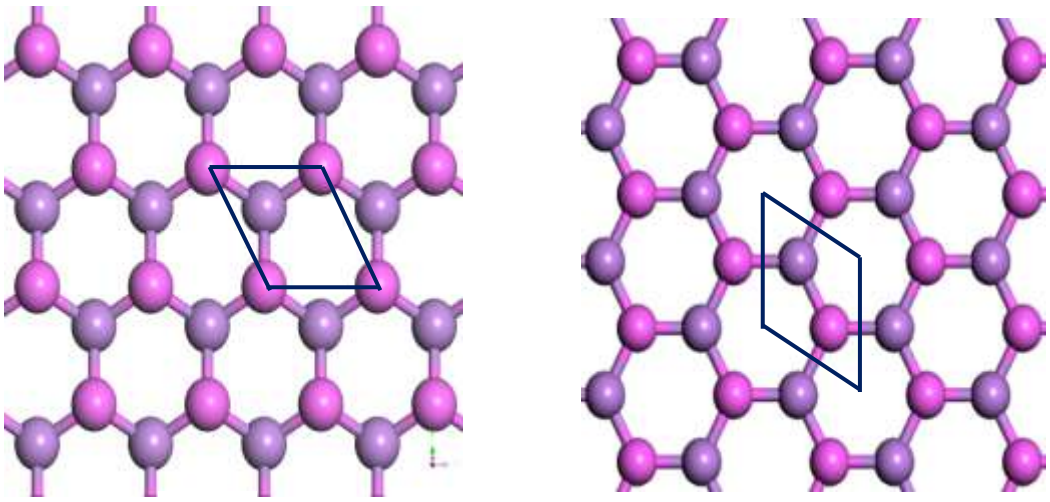

(a) (b)

Figure 1: Crystal structure of MAlAs (a) Buckled and (b) planar. The unit cell of a MAlAs crystal, marked by a parallelogram.

The third step was the computation of elastic constants to analyse mechanical stability. The three major independent elastic constants (C11, C12, and C66) can be employed to determine 2D hexagonal structure elastic characteristics [23]. The two well-known mechanical stability criteria for a hexagonal structure are C66 > 0 and |C12| < C11. As shown in Table 1, these elastic parameters met the required characteristics of hexagonal monolayer structure to be stable and it indicates the possibility of fabricating MAlAs. According to the results of these three steps, although the negative phonon modes prefer to the instability of MAlAs under mechanical deformation, the large values of cohesive energy and proper elastic constant parameters nominate MAlAs to be experimentally synthesized.

Table 1: The computational results in this study of the structural, mechanical and electronic parameters of planar and buckled MAlAs

property		Planar MAlAs	Buckled MAlAs
Lattice const. a (A°)		4.03	4.014
Bond length (A°)		2.33	2.34
Buckling height (A°)		0.00	0.32
Angles α=β, ϒ		90, 120	90, 120
Cohesive energy (eV)		5.04	5.08
C11		10.29	8.64
C12		4.69	2.79
C66		2.80	2.92
Fermi level (eV)		-5.68	-4.67
Indirect Eg (eV) (K→G)		2.45	2.67
m_h^* (m_o)	G	0.81	0.79
	K	0.67	0.67

m_e^* (m_o)	M	0.99	0.90
	G-K	0.71	1.41
	G-M	1.41	1.45
	G	0.15	0.14
	K	0.77	0.87
	M	0.17	0.43
	G-K	0.28	0.31
	G-M	0.28	0.31

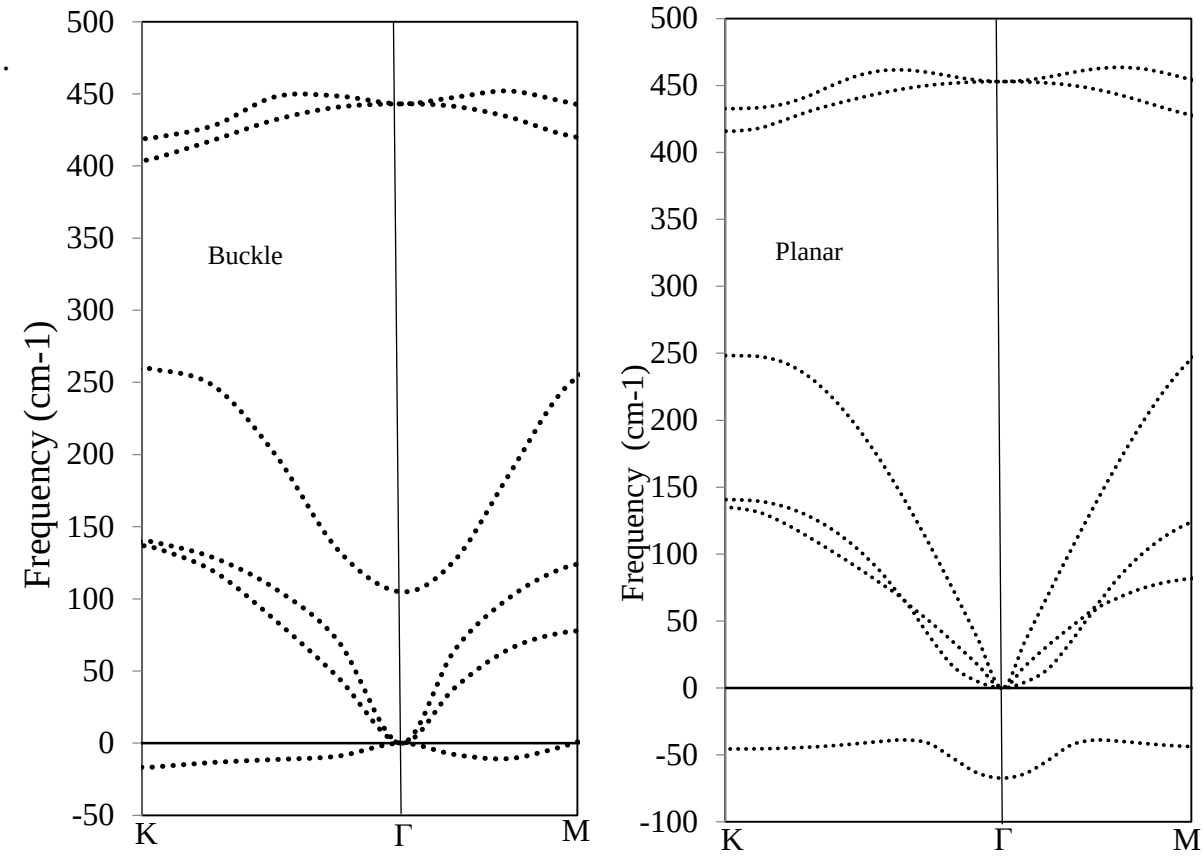

Figure 2: Phonon dispersion band structure of planar and buckled MAlAs.

Figure 3 reviews the fermion dispersion of the MAlAs. The fermions band structure is shown in the first Brillouin zone along the lines Γ–K–M–Γ of high symmetry points for planar and buckled MAlAs computed by the HSE06 method. It is evident that planar and buckled MAlAs have indirect band gap of 2.45 and 2.67 eV, respectively. Thus, MAlAs is a semiconductor. The semiconductor indirect band gap characteristic presents the top edge of the valence band at the K symmetry point while the bottom of the conduction band is at the Γ symmetry point. The partial density of states (PDOS) was calculated to probe the electronic properties. The conduction band consist of a strong hybridization of 3s and 3p bands of Al atoms. The 4p bands of As atoms are located below the 3p bands of Al atoms separated by a band gap. The electronegativity disproportion between Al and As atoms in MAlAs initiates a gapped phase, moreover, massive Dirac fermions play a role in setting the optical and electronic transport properties. Table 1 shows the effective masses estimated using a second derivative of the five-point method. To eliminate the effect of non-parabolic errors, a k-point

difference is made much smaller than $0.001^{\circ}A^{-1}$. The effective mass toward ΓK show different values from those along the ΓM direction. The proportional electron effective mass is small and the hole effective mass is excessively large. According to the results, the planar/buckled MAlAs has anisotropic/isotropic hole effective mass, while the systems have isotropic electron effective mass. As shown in Table 1, planar MAlAs is seen to have hole effective mass of (1.41 m_o) in the G-K direction which is larger than that of the G-M direction of (0.71 m_o), where m_o is the electron rest mass.

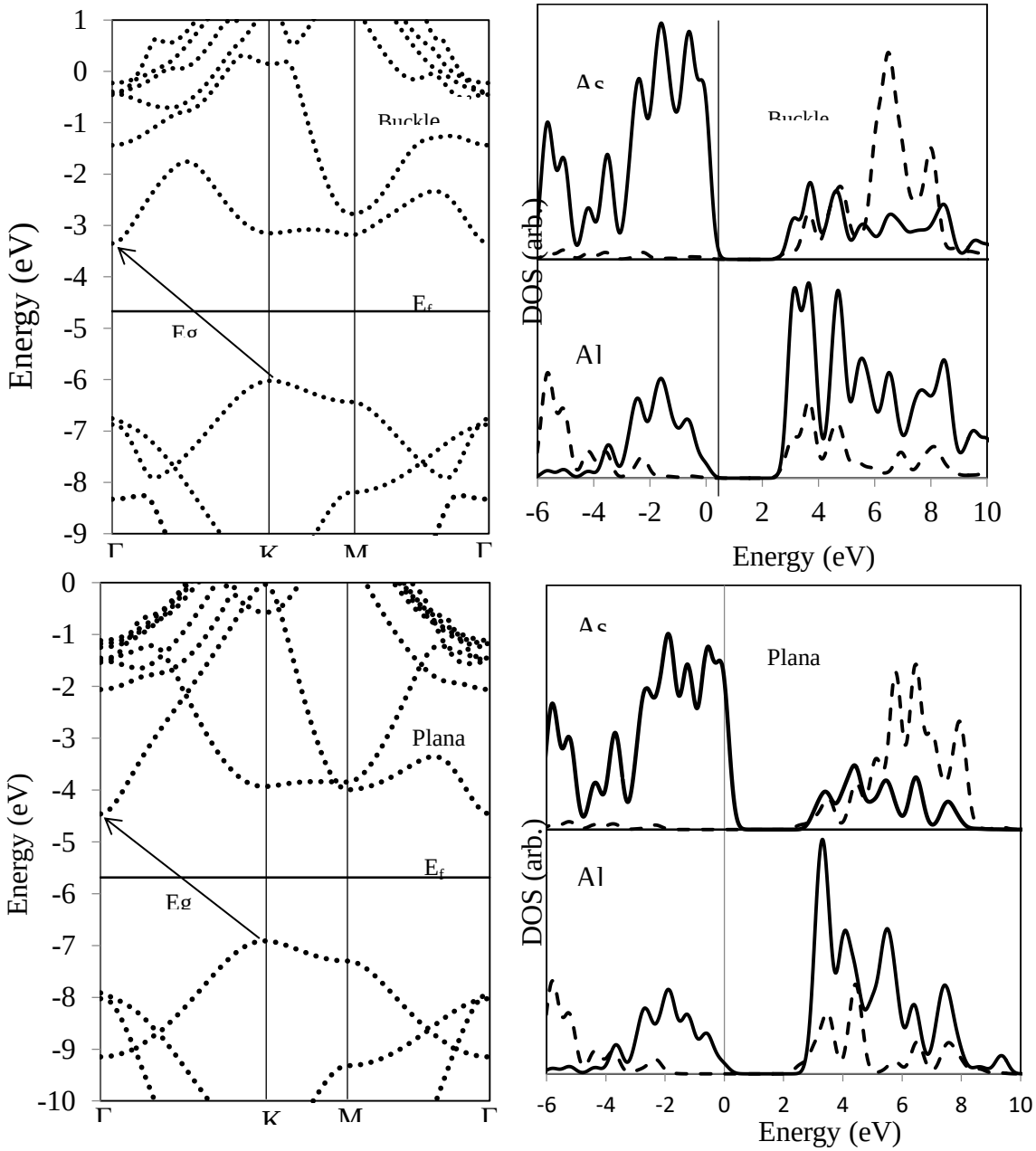

Figure 3: The electronic band structure and density of states for planar and buckled MAlAs.

The visible absorption spectrum of materials is an important optical property. Therefore, the absorbance was computed using the PBE function. As shown in Figure 4, prominent strong (~10^4 cm^{-1}) peaks has showed up in the energy range between 2.5 eV and 8 eV. This indicates that MAlAs have absorption of both visible light wavelengths in addition to the absorption of high energetic frequency of UV light. The absorption coefficient levels off at

about 2.8 eV, that corresponds to the indirect absorption. At 3.5 eV, the absorption coefficient again increases, which is the onset of direct absorption.

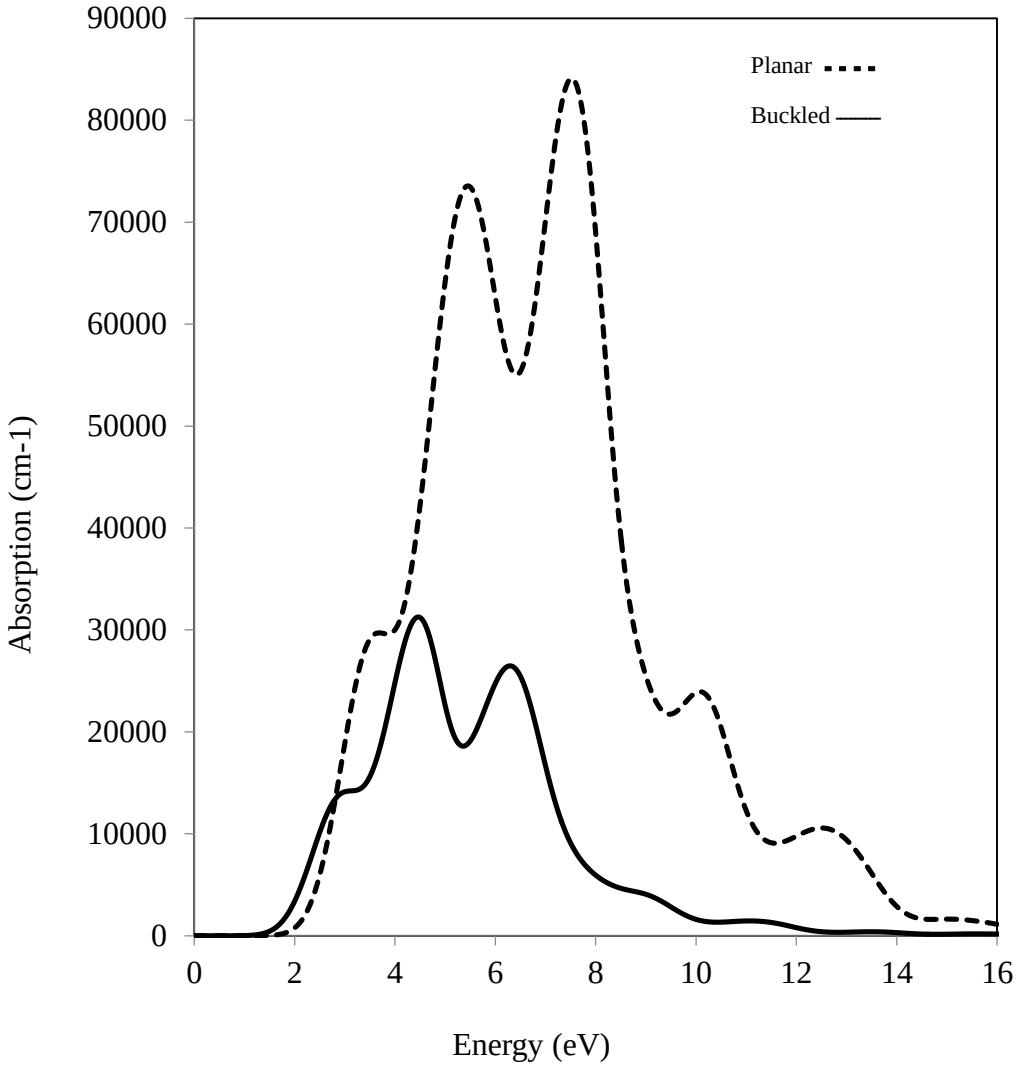

Figure 4: The absorption spectra of planar and buckled MAlAs.

4. Conclusions

In this work, the first principle computations are accomplished for predicting structural, mechanical, electronic and optical properties of planar and buckled hexagonal AlAs monolayer. It has approached low kinetic stability according to the phonon dispersion, cohesive energy and results of elastic constants. The visible absorption spectrum showed that absorption coefficient levels off at about 2.8 eV, which corresponds to indirect absorption. At 3.5 eV, the absorption coefficient again increases, which is the onset of direction absorption. In relation to the theoretical results, AlAs monolayer is seen to has an indirect band gap (~2.56 eV). Furthermore, the AlAs monolayer has to some extent good absorption coefficient (~10^4 cm^{-1}) in the visible range; it also has absorption in the ultraviolet region.

References

[1] D. Akinwande, C. Huyghebaert, C. Wang, M. I. Serna, S. Goossens, L. Li, H. P. Wong and F.H. L. Koppens, "Graphene and two-dimensional materials for silicon technology," *Nature*, vol. 573, no. 7775, pp. 507-518, 2019.

[2] A. Mohsin Ali, "A Electron transport study on ultrathin armchair graphene nanoribbone," *Journal of Kufa-Physics*, vol. 11, no. 2, pp. 62-72, 2019.

[3] L. Yang, W. Cheng, Q. Yu and B. Liu, "Mass production of two-dimensional materials beyond graphene and their applications," *Nano Research*, vol. 14, no. 6, pp. 1583-1597, 2021.
[4] T. Suzuki, "Theoretical discovery of stable structures of group III-V monolayers:The materials for semiconductor devices," *Applied Physics Letters*, vol. 107, p. 213105, 2015.
[5] H. K. Abdul-Rassol and A. M. Abdul-Hussein, "Manufacture a Battery-like Supercapacitors with Electrodes of Graphene," *Iraqi Journal of Science*, vol. 58, no. 3C, pp. 1694-1707, 2017.
[6] A. M. Ali and A. M. AlMowali, "Ab initio Study of the Electronic and Optical Properties of Stable Boron Sheet," *Iraqi Journal of Science*, vol. 62, no. 12, pp. 4687-4693, 2021.
[7] H. Şahin, S. Cahangirov, M. Topsakal, E. Bekaroglu, E. Akturk, R. T. Senger and S. Ciraci, "Monolayer honeycomb structures of group-IV elements and III-V binary compounds: First-principles calculations," *Physical Review B*, vol. 80, no. 15, p. 155453, 2009.
[8] X. Zhang, Z. Liu and S. Hark, "Synthesis and optical characterization of single-crystalline AlN nanosheets," *Solid state communications*, vol. 143, no. 6-7, pp. 317-320, 2007.
[9] S. Valedbagi, A. Fathalian and S. M. Elahi, "Electronic and optical properties of AlN nanosheet: an ab initio study," *Optics Communications*, vol. 309, pp. 153-157, 2013.
[10] M. Yarmohammadi and K. Mirabbaszadeh "Electric field tuning of the properties of monolayer hexagonal boron phosphide," *Journal of Applied Physics*, vol. 128, no. 21, p. 215703, 2020.
[11] L. A. Cipriano, G. Di Liberto, S. Tosoni and G. Pacchioni, "Quantum confinement in group III–V semiconductor 2D nanostructures," *Nanoscale*, vol. 12, no. 33, pp. 17494-17501, 2020.
[12] B. Monemar, "Fundamental energy gaps of AlAs and AlP from photoluminescence excitation spectra," *Physical Review B*, vol. 8, no. 12, p. 5711, 1973.
[13] H. Jin, G. L. Zhao and D. Bagayoko, "Density functional band gaps of AlAs," *Physical Review B*, vol. 73, no. 24, p. 245214, 2006.
[14] I. Itskevich, S. I. Rybchenko, I. I. Tartakovskii, S. T. Stoddart, A. Levin, P. C. Main, L. Eaves, M. Henini and S. Parnell, "Stark shift in electroluminescence of individual InAs quantum dots," *Applied Physics Letters*, vol. 76, no. 26, pp. 3932-3934, 2000.
[15] J. Jiang, Y. Li, F. Chang, S. Cui, W. Chen, D. Jiang, G. Wang, Y. Xu, Z. Niu, R. Che, C. Zhang and L. Huang, "MBE growth of mid-wavelength infrared photodetectors based on high quality InAs/AlAs/InAsSb superlattice," *Journal of Crystal Growth*, vol. 564, p. 126109, 2021.
[16] G. Sinatkas, T. Christopoulos, O. Tsilipakos and E. E. Kriezis, "Electro-optic modulation in integrated photonics," *Journal of Applied Physics*, vol. 130, no. 1, p. 010901, 2021.
[17] V. Villafane, P. Sesin, P. Soubelet, S. Anguiano, A. E. Bruchhausen, G. Rozas, C. Gomez Carbonell, A. Lemaître, and A. Fainstein, "Optoelectronic forces with quantum wells for cavity optomechanics in GaAs/AlAs semiconductor microcavities," *Physical Review B*, vol. 97, no. 19, p. 195306, 2018.
[18] I. Vurgaftman and J. R. Meyer, "Band parameters for III–V compound semiconductors and their alloys," *Journal of applied physics*, vol. 89, no. 11, pp. 5815-5875, 2001.
[19] S. J. Clark, M. D. Segall, C. J. Pickard, P. J. Hasnip, M. I. J. Probert, K. Refson, and M. C. Payne, "First principles methods using CASTEP," *Zeitschrift für kristallographie-crystalline materials*, vol. 220, no. 5-6, pp. 567-570, 2005.
[20] A. J. Mannix, X. Zhou, B. Kiraly, J. D. Wood, D. Alducin, B. D. Myers, X. Liu, B. L. Fisher, U. Santiago, J. R. Guest, M. J. Yacaman, A. Ponce, A. R. Oganov, M. C. Hersam and N. P. Guisinger, "Synthesis of borophenes: Anisotropic, two-dimensional boron polymorphs," *Science*, vol. 350, no. 6267, pp. 1513-1516, 2015.
[21] J. P. Perdew, K. Burke and M. Ernzerhof, "Generalized gradient approximation made simple," *Physical review letters*, vol. 77, no. 18, p. 3865, 1996.
[22] J. Heyd, G. E. Scuseria, and M. Ernzerhof, "Hybrid functionals based on a screened Coulomb potential," *The Journal of chemical physics*, vol. 118, no. 18, pp. 8207-8215, 2003.
[23] C. J. Pethick, Z. Zhang and D. N. Kobyakov, "Elastic properties of phases with nonspherical nuclei in dense matter," *Physical Review C*, vol. 101, p. 055802, 2020.